SUPPLEMENTAL MATERIAL

Imaging the vascular bone marrow niche during inflammatory stress

Katrien Vandoorne DVM PhD[1*], David Rohde MD[1*], Hye-Yeong Kim PhD[1], Gabriel Courties PhD[1], Gregory Wojtkiewicz MEng[1], Lisa Honold PhD[1], Friedrich Felix Hoyer MD[1], Vanessa Frodermann PhD[1], Ribhu Nayar PhD[1], Fanny Herisson PhD[1], Yookyung Jung PhD[1,2], Pauline A. Désogère PhD[3], Claudio Vinegoni PhD[1], Peter Caravan PhD[3], Ralph Weissleder MD PhD[1,4], David E. Sosnovik PhD[3,5], Charles P. Lin PhD[1,2], Filip K. Swirski PhD[1], Matthias Nahrendorf MD PhD[1,5]

[1]Center for Systems Biology and Department of Imaging, Massachusetts General Hospital and Harvard Medical School, Boston, MA.
[2]Wellman Center for Photomedicine, Massachusetts General Hospital and Harvard Medical School, Boston, MA.
[3]Martinos Center for Biomedical Imaging, Department of Radiology, Massachusetts General Hospital and Harvard Medical School, Charlestown, MA.
[4]Department of Systems Biology, Harvard Medical School, Boston, MA.
[5]Cardiovascular Research Center, Massachusetts General Hospital and Harvard Medical School, Charlestown, MA.

*These authors contributed equally to this work.

Detailed Methods

Intravital fluorescent agents

OsteoSense® 750EX (4 nmol/mouse, NEV10053EX, PerkinElmer) enriches in osteoblasts located at the bone surfaces of the calvaria[1]. IntegriSense™ 680, as an angiogenic marker, was administered intravenously 24 hours prior to imaging (2 nmol/mouse, NEV10645, PerkinElmer). IntegriSense is a selective non-peptide small molecule integrin αvβ3 antagonist and an NIR fluorochrome. This agent enables in vivo visualization and quantification of integrin αvβ3 expression in neovasculature[2,3].

PET/MRI data analysis

For albumin-based DCE-MRI, pixel-by-pixel basis with Matlab R2015b software (MathWorks Inc., Natick, MA) to derive concentrations of RhoB-albumin-GdDTPA for the selected slice in the dynamic datasets were calculated as described before[4, 5]. Entire femurs were drawn as ROIs. Mean femoral R_1 values (R_{1pre}; $R_1 = 1/T_1$) precontrast and postcontrast were calculated using variable flip angle (α) data by nonlinear best fit to Equation 1:

$$I = \frac{M_0 \sin\alpha (1 - e^{-TR \cdot R_{1pre}})}{1 - \cos\alpha \cdot e^{-TR \times R_{1pre}}} \qquad [1]$$

where I is the signal intensity as a function of the pulse flip angle α, TR is the repetition time (25ms) and the pre−exponent term M_0 includes the spin density and T_2 relaxation effects, assumed to be unaffected by the contrast agent. Postcontrast R_1 values were calculated from signal intensities precontrast and postcontrast (I_{pre} and I_{post}; Equation 2):

$$\frac{I_{pre}}{I_{post}} = \frac{M_0 \sin\alpha (1 - e^{-TR \cdot R_{1pre}}) / (1 - \cos\alpha \cdot e^{-TR \cdot R_{1pre}})}{M_0 \sin\alpha (1 - e^{-TR \cdot R_{1post}}) / (1 - \cos\alpha \cdot e^{-TR \cdot R_{1pre}})} \qquad [2]$$

Lastly, concentrations of the contrast agent were derived from the measured *relaxivity* (*R*) of RhoB-albumin-GdDTPA (*R*= 145mM/s ;Equation 3):

$$[RhoB\text{-}albumin\text{-}GdDTPA] = \frac{1}{R}\,(R_{1post} - R_{1pre}) \qquad [3]$$

Histology and immunostaining

For histology, the hypoxia probe pimonidazole (HP2-200Kit, Hypoxyprobe Inc.) was intraperitoneally injected (60 mg/kg) 2 h before euthanasia. Femurs were dissected and fixed in 4% paraformaldehyde (PFA), then decalcified in EDTA 20% with shaking at 4°C for 2 weeks. Femurs were transferred to 30% sucrose/PBS at 4°C for 2 days, incubated in equal volume OCT/30% sucrose overnight, embedded in OCT and then sectioned longitudinally at 5µm thickness. For immunostaining, femur sections were stained with endomucin (anti-rabbit, abcam, ab106100; anti-goat, Novus Biologicals, AF4666); ki67 (anti-rat, Abcam, ab15580); integrin αVβ3 (anti-rabbit, Abbiotec, 251672) and/ or FITC-conjugated anti-pimonidazole (HP2-200Kit, Hypoxiprobe Inc.) overnight. Primary antibodies were conjugated with secondary antibodies (Thermofischer Scientific; Donkey anti-Rat IgG AF488, A21208; Donkey anti-Rabbit IgG AF 546, A10040; Donkey anti-goat IgG AF 680, A21084) to amplify the signal, and nuclei were stained with DAPI (4',6-diamino-2-phenylindole) (Sigma). Femur sections were stained with H&E and scanned with NanoZoomer 2.0-RS (Hamamatsu) at 40× magnification. Histological fluorescent images were imaged with a Nikon 80i (Nikon) and analyzed using ImageJ software. Regions of interest (ROIs) were defined to avoid quantification within regions with folded tissue or high background staining and to restrict analysis to bone marrow (BM) regions of the distal metaphysis of the femur. The percent area fluorescent endomucin staining in each field of view was calculated using ImageJ software; the same threshold was applied to all samples (three to five sections/animal). Endothelial area was defined as stained cells only. Average endothelial area per vessel was quantified. Results are aggregated per animal.

ELISA

Blood and femur samples were collected. The blood was then centrifuged for 20 min at 2,000 x g, and serum was gathered within 30min of initial collection. Femur BM was acquiredby centrifuging femurs for 20 min at 12,000 x g prior to the procedure. Quantitative measurement of vascular endothelial growth factor (VEGF; Mouse VEGF Quantikine ELISA Kit, R&D) and angiopoetin-1 (ANGPT1; Mouse ANGPT1 ELISA Kit, LSBio) in the serum and bone marrow were determined according to manufacturers' protocols.

Cell sorting and flow cytometry

For flow and sort of endothelial cells and $CD45^+$ cells, bone marrow cells were flushed from femurs and digested with 1 mg ml^{-1} collagenase IV (Sigma) and 2 mg ml^{-1} dispase II (Gibco) in Dulbecco's Modified Eagle's Medium without phenol red (Sigma) at 37°C for 30min. Debris and dead cells were excluded by FCS, SSC and DAPI (4',6-diamino-2-phenylindole) (FxCycleTM Violet stain, Life Technologies) staining profiles. Samples were recorded on a LSRII flow cytometer equipped with FACS Diva 6.1 software (BD) and data were analyzed with FlowJo 10 software (Tree Star). All cell-sorting experiments were performed using an Aria Cell Sorter (BD Biosciences). For endothelial cells or $CD45^+$ cell surface marker staining, BV605/ ApcCy7 anti-Ter119 (TER-119, 116239/116223); PerCP/Cy5.5 anti-CD41 (MWReg30, 133918); phycoerythrin (PE) anti-CD31 (MEC13.3, 102408) PE/Cy7 anti-Sca1 (D7, 108114) (all from Biolegend); fluorescein isothiocyanate (FITC) anti-CD45.2 (104, 553772, BD Pharmingen); IntegriSense™ 680 (in vivo injected 100µl- 2h before sacrificing PerkinElmer, NEV10645) were used in this study. Bone marrow $Ter119^-CD45^-CD31^{high}$ endothelial cells and $CD41^-Ter119^-CD45^+$ cells were

identified (Supplemental fig. S4). Cell numbers per femur were calculated as total cells per femur sample multiplied by percentage of cells obtained from the live cell FACS gate.

For cell cycle analysis, cells were stained for endothelial cells or $CD45^+$ cell surface markers as described above, then fixed and permeabilized using the Foxp3/Transcription Factor Staining Buffer Set (eBioscience) according to manufacturer's instructions. Cells were then stained with eFluor 660-anti-Ki67 (SolA 15, 50-5698-82) and isotope eFluor 660-anti-Rat IgG2a (50-4321-80) (both from BioScience).

For LSK sorts, cells from n=5 mice were pooled to obtain enough LSKs for one adoptive transfer. The marrow of humerus, tibia and femurs was collected by flushing. The obtained suspension was then filtered through a 40 µm cell stainer into a 50 ml Falcon tube. Bone marrow cells were stained with biotin conjugated antibodies against lineage markers including B220 (RA3-6B2, 103204); CD3ε (145-2C11, 100304); CD4 (GK1.5, 100404); CD8α (53-6.7, 100704); CD11b (M1/70, 101204); CD11c (N418, 117304); Gr-1 (RB6-8C5, 108404); NK1.1 (PK136, 108704); Ter119 (TER-119, 116204) followed by streptavidin BV605 (405229) conjugates and antibodies against APC anti-cKit (2B8, 105812); PE/Cy7 anti-Sca-1 (D7, 108114) (all from Biolegend) and DAPI. LSK were identified as $Lin^-Sca\text{-}1^+c\text{-}Kit^+$ as described before[2].

RNA isolation and quantitative PCR
Bone marrow cells were sorted according to their specific flow cytometric profiles. RNA was purified using a PicoPure RNA Isolation Kit (Thermofisher Scientific, KIT 0204). A high capacity RNA-to-cDNA kit was used to generate cDNA (cat:4387406, Applied Biosystems). Taqman Fast Universal PCR Mastermix was used for qPCR (cat:4352042 Applied Biosystems). All Primers were TaqMan® Primer purchased from Applied Biosystems.

Transmission Electron Microscopy
Decalcified distal metaphysis femurs containing intact bone marrow were cut into small pieces and immersion-fixed in PFA 4%, rinsed several times in 0.1M sodium cacodylate buffer and post-fixed in 2.5% glutaraldehyde in 0.1M sodium cacodylate buffer (pH 7.4, Electron Microscopy Sciences, Hatfield, PA) for 2hr at room temperature on a gentle rotator. Fixative was further allowed to infiltrate 24-48hr at 4°C. Tissue blocks were rinsed several times in 0.1M sodium cacodylate buffer, post-fixed in 1.0% osmium tetroxide in cacodylate buffer for one hour at room temperature and rinsed several times in cacodylate buffer. Specimens were then dehydrated through a graded series of ethanols to 100% and dehydrated briefly in 100% propylene oxide. Samples were allowed to pre-infiltrate 2hrs in a 2:1 mix of propylene oxide and Eponate resin (Ted Pella, Redding, CA) then transferred into a 1:1 mix of propylene oxide and Eponate resin and allowed to infiltrate overnight on a gentle rotator. The following day, specimens were transferred into a 2:1 mix of Eponate resin and propylene oxide for a minimum of 2hrs, then allowed to infiltrate in fresh 100% Eponate resin for several hours more; tissue blocks were embedded in flat molds with fresh 100% Eponate and allowed to polymerize 24-48hrs at 60°C. Thin (70nm) sections were cut using a Leica EM UC7 ultramicrotome, collected onto formvar-coated grids, stained with uranyl acetate and Reynold's lead citrate and examined in a JEOL JEM 1011 transmission electron microscope at 80 kV. Images were collected using an AMT digital imaging system with proprietary image capture software (Advanced Microscopy Techniques, Danvers, MA).

PET agent
NODAGA-RGD trifluoroacetate (cyclo[-Arg-Gly-Asp-D-Tyr-Lys(NODAGA)-]) was purchased from ABX Advanced Biochemical Compounds. All other reagents were purchased from Sigma-Aldrich and used without further purifications, unless otherwise stated. 68GaCl3 was obtained from 68Ge/68Ga generator (ITG) and eluted with 0.1 M HCl. 68GaCl3 eluent (~10-14 mCi) was

diluted with sodium acetate buffer (3 M, pH 5) to equilibrate to pH ~4. NODAGA-RGD (30 µg, 30.7 µmol) was dissolved with 0.1 M ammonium acetate buffer (100 µL, pH 6) and combined with 68GaCl3. The labeling mixture was heated at 80°C for 10 min on a thermomixer (900 rpm). The mixture was loaded on a C18 Sep-Pak plus cartridge (Waters, WAT020515), and the labeled product was eluted with 1.5 mL ethanol followed by dying at 65 °C with a gentle argon stream. The final formulation was adjusted to ~3% ethanol in saline. Analytical radio-HPLC demonstrated >99% radiochemical purity using Agilent 1260 Infinity. The C-18 reverse-phase analytical column (Agilent Proshell 120, 2.7 µm, 4.6 X 50 mm, 2 mL/min) was used with a 5% to 95% gradient of solvent B 0.1 % formic acid in acetonitrile and solvent A 0.1 % formic acid in water over 10 min. Specific activity was ~8.02 GBq/µmol with a ~72% radiochemical yield.

Gamma counting and autoradiography

After ^{68}Ga-NODAGA-RGD injection, mice were sacrificed and the direct γ counting was performed on the aortic root, the spleen and a femur using a gamma counter (1480 Wizard 3", PerkinElmer, Boston, MA). The data are presented as percent injected dose per gram of tissue (%IDGT). After ^{68}Ga-NODAGA-RGD PET imaging, femurs from both control and LPS-treated mice were excised and exposed for autoradiography on the PhosphorImager (Amersham Typhoon 9410 Biomolecular Imager, GE Healthcare, Boston, MA) for 24 hours.

Statistics

Statistical analyses were performed using GraphPad Prism 7 software (GraphPad Software, Inc.). Results are reported as mean ± standard error of mean (sem). Normality was assessed using D'Agostino-Pearson normality test. For a two-group comparison, normally distributed datasets underwent a parametric t-test, whereas non-normally distributed data were evaluated with a nonparametric Mann-Whitney test. To compare three groups, a one-way ANOVA test, followed by nonparametric Kruskal-Wallis test, was applied for non-normally distributed data. For quantitative PCR, two-way ANOVA was performed, followed by Holm–Sidak test for multiple comparisons.

REFERENCES

1. Courties G, Herisson F, Sager HB, Heidt T, Ye Y, Wei Y, Sun Y, Severe N, Dutta P, Scharff J, Scadden DT, Weissleder R, Swirski FK, Moskowitz MA, Nahrendorf M. Ischemic stroke activates hematopoietic bone marrow stem cells. *Circ Res*. 2015;116:407-417.
2. Snoeks TJ, Löwik CW, Kaijzel EL. In vivo optical approaches to angiogenesis imaging. *Angiogenesis*. 2010;13:135-147.
3. Leuschner F, Rauch PJ, Ueno T, Gorbatov R, Marinelli B, Lee WW, Dutta P, Wei Y, Robbins C, Iwamoto Y, Sena B, Chudnovskiy A, Panizzi P, Keliher E, Higgins JM, Libby P, Moskowitz MA, Pittet MJ, Swirski FK, Weissleder R, Nahrendorf M. Rapid monocyte kinetics in acute myocardial infarction are sustained by extramedullary monocytopoiesis. *J Exp Med*. 2012;209:123-137.
4. Vandoorne K, Vandsburger MH, Jacobs I, Han Y, Dafni H, Nicolay K, Strijkers GJ. Noninvasive mapping of endothelial dysfunction in myocardial ischemia by magnetic resonance imaging using an albumin-based contrast agent. *NMR Biomed*. 2016;29:1500-1510.
5. Aychek T, Vandoorne K, Brenner O, Jung S, Neeman M. Quantitative analysis of intravenously administered contrast media reveals changes in vascular barrier functions in a murine colitis model. *Magn Reson Med*. 2011;66:235-243.

SUPPLEMENTAL FIGURES

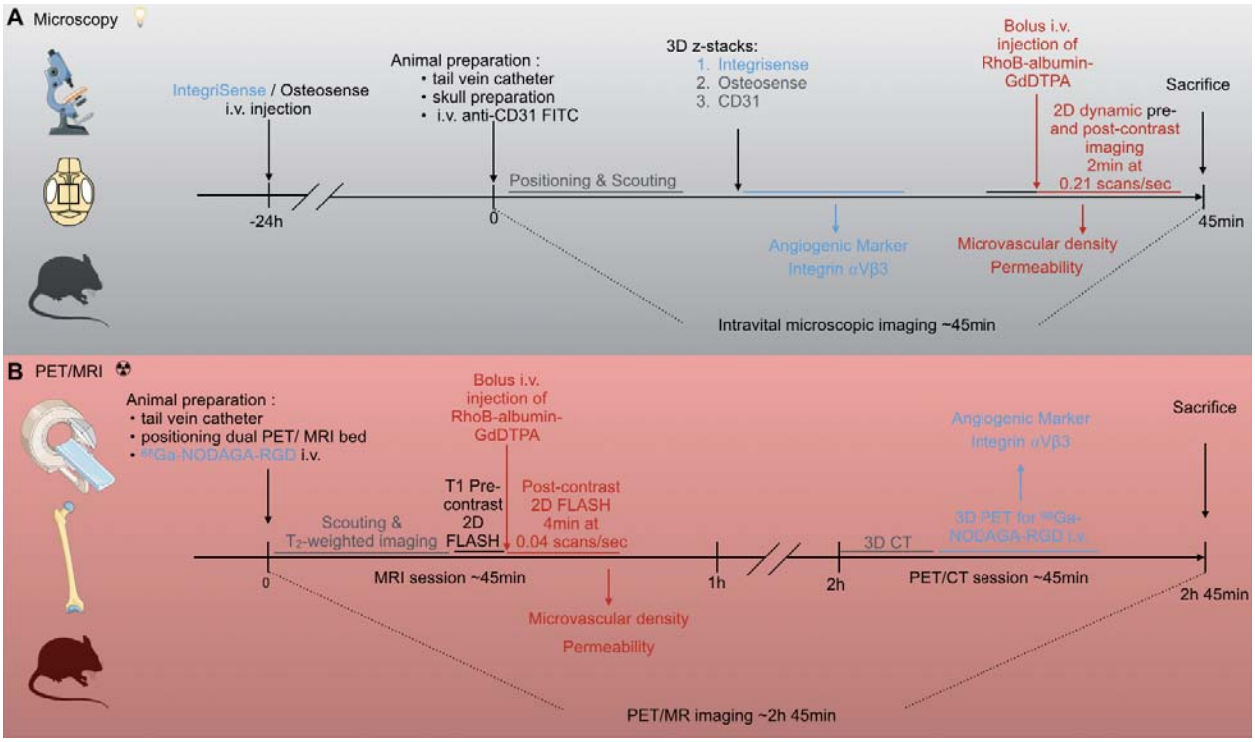

Online Figure I. Experimental design of (A) intravital microscopic imaging and (B) PET/MR imaging.

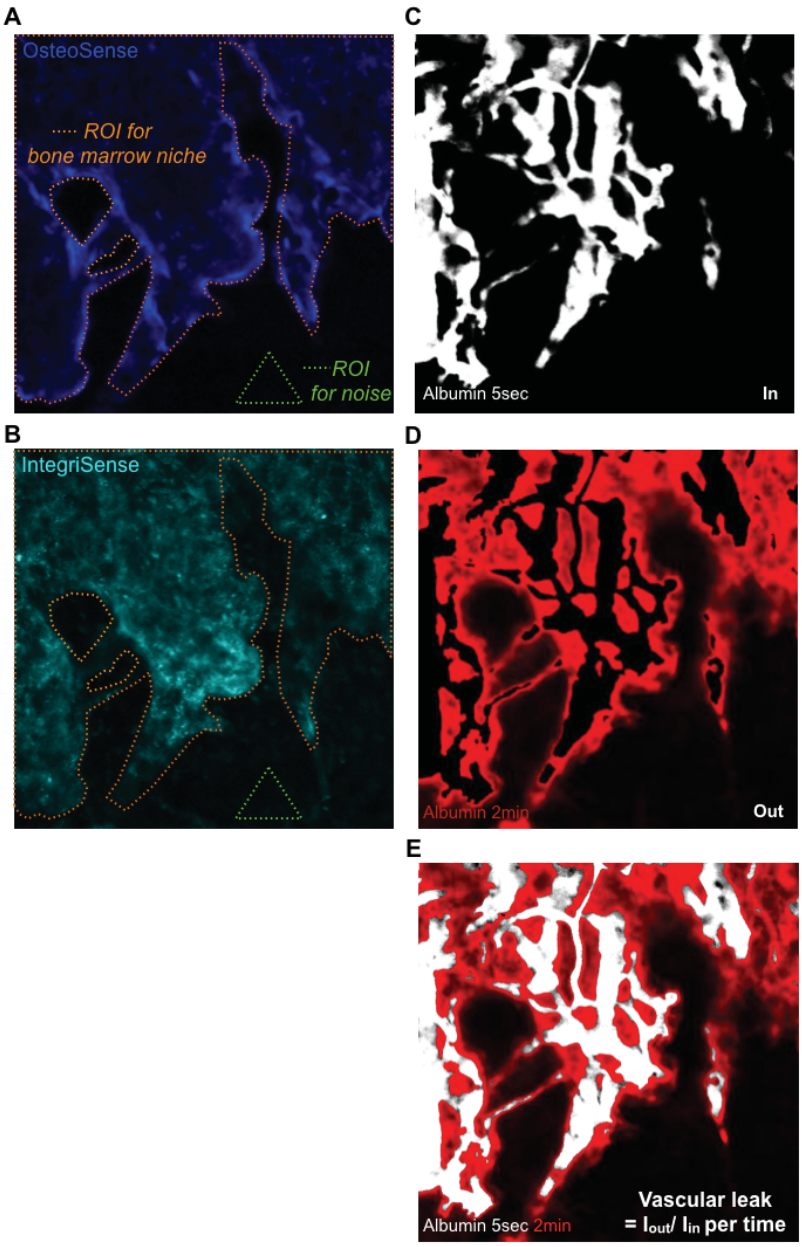

Online Figure II. Quantification of bone marrow vascular features. **(A)** Region of interest (ROI) for the bone marrow niche (orange dotted line) according to OsteoSense signal. The resulting area was used for analysis of both, IntegriSense and vascular leak. A ROI for background (green dotted triangle) was chosen in an osseous region without OsteoSense signal. **(B)** Maximum intensity projection of a z-stack with 16 slices was used to quantify target (ROI in bone marrow niche) to background (ROI for background). **(C)** Dynamic albumin imaging t=5sec. The data derived from the initial signal (t=5sec) are used to quantify vascular density in the bone marrow niche after albumin injection. **(D)** Dynamic albumin imaging t=2min. The blood vessels' outline from the initial signal (C; t=5sec) is used to differentiate the signal derived from the albumin inside and outside the vasculature. **(E)** Vascular leak is shown as a ratio of intensity signal OUT/IN per time.

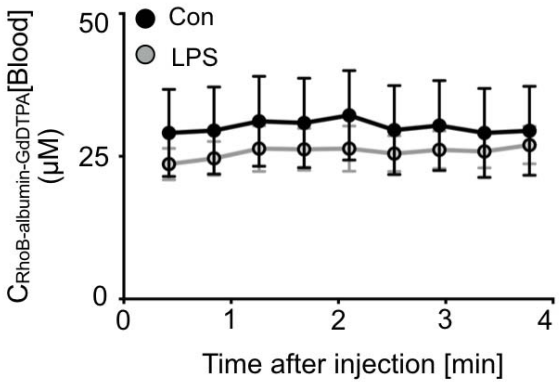

Online Figure III. Blood RhoB-albumin-GdDTPA concentration after i.v. injection derived from a ROI placed in the vena cava.

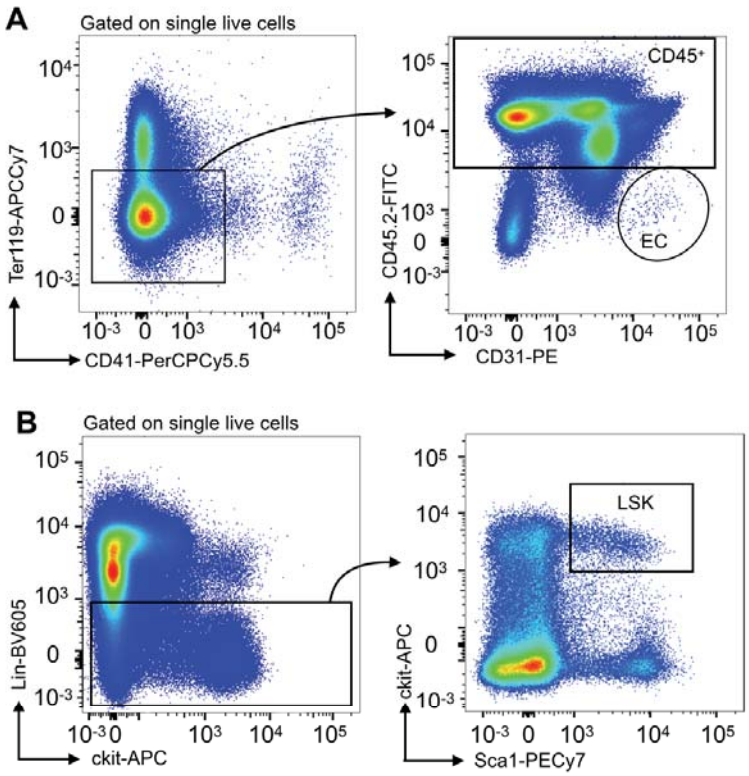

Online Figure IV. Gating strategies for bone marrow. (**A**) Gating strategy for bone marrow endothelial cells (EC) and $CD45^+$ cells. (**B**) Gating strategies for sorting $Lin^-Sca1^+Kit^-$ cell (LSK) to be adoptively transferred.

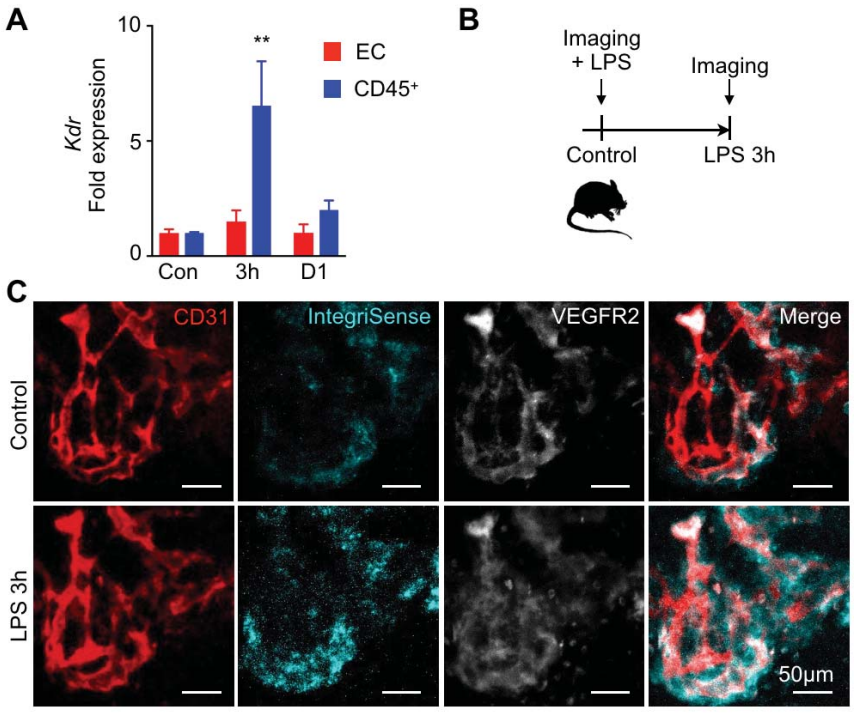

Online Figure V. Vascular endothelial growth factor receptor 2 (VEGFR2) after TLR ligand stress. (**A**) *Kdr* mRNA expression (encoding for VEGFR2) in sorted endothelial cells (EC) and CD45$^+$ leukocytes of bone marrow harvested from control mice (con, n=5) and treated mice 3h (3h, n=5) and 1 day (D1, n=4) after intraperitoneal LPS injection. (**B**) Mice were imaged before and 3h after LPS. (**C**) Intravital images comparing CD31$^+$ vessels, IntegriSense signal and VEGFR2 in the calvaria. Mean ± sem; two-way ANOVA followed by Holm–Sidak test for multiple comparisons; ** P<0.01.

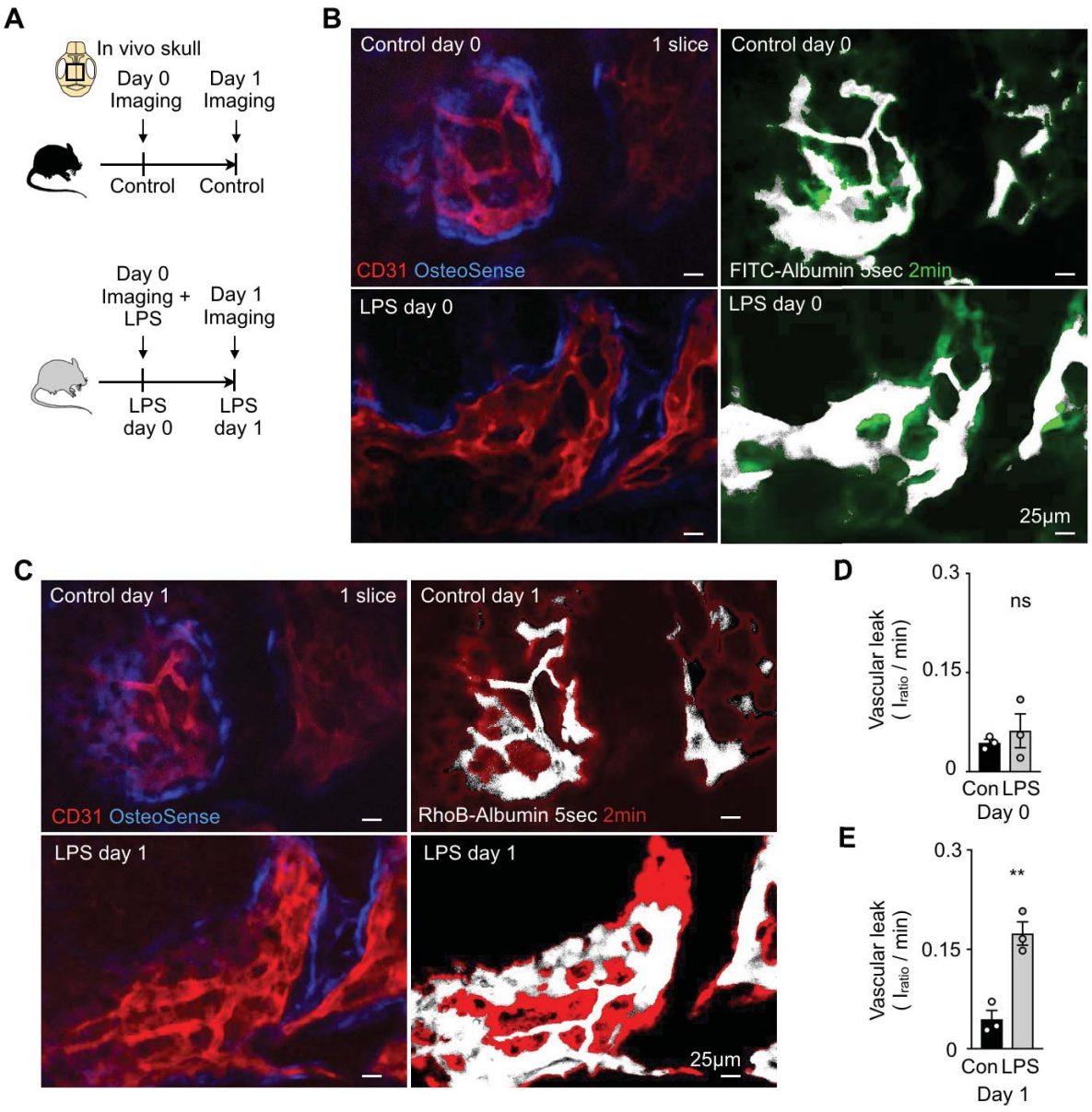

Online Figure VI. (**A**) Experimental outline. (**B, C**) Serial imaging of marrow niche permeability (B) before and (C) 1 day after LPS injection. Controls were imaged on two consecutive days. (**D,E**) Permeability measurements via serial imaging of the bone marrow niche**.** Control mice (con; n=3) and LPS-treated mice (LPS; n=3); mean ± sem; Unpaired t-test; ns = not significant; ** P<0.001**.**

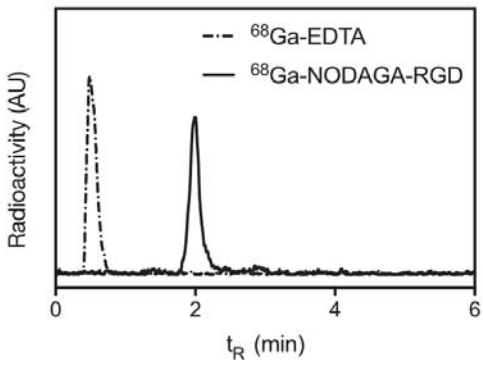

Online Figure VII. Radio HPLC chromatograms of ^{68}Ga-labeled NODAGA-RGD (solid line) and free ^{68}Ga chelated with EDTA (dotted line). ^{68}GA-NODAGA-RGD elutes at ~2.1 min with no detectable unchelated ^{68}Ga, indicating >99% radiochemical purity of the PET imaging agent.

Legends for video files

Online video I (control) and II (LPS): In vivo intravital microscopy of the skull documenting increased IntegriSense signal in calvaria of LPS-treated mice. The movies show a z-stack.